

Two-photon interferometry for high-resolution imaging

DMITRY V. STREKALOV* and JONATHAN P. DOWLING

Quantum Computing Technologies Group, Jet Propulsion Laboratory,
California Institute of Technology, MS 300-123, 4800 Oak Grove
Drive, Pasadena, CA 91109, USA

(Received 15 March 2001; revision received 15 June 2001)

Abstract. This paper discusses the advantages of using non-classical states of light for two aspects of optical imaging: the creation of microscopic images on photosensitive substrates, which constitutes the foundation for optical lithography, and the imaging of microscopic objects. In both cases, the classical resolution limit given by the Rayleigh criterion is approximately half of the optical wavelength. It has been shown, however, that by using multi-photon quantum states of the light field, and a multi-photon sensitive material or detector, this limit can be surpassed. A rigorous quantum mechanical treatment of this problem is given, some particularly widespread misconceptions are addressed, and turning quantum imaging into a practical technology is discussed.

The idea of overcoming the limits of classical optical imaging by using multi-photon processes is fairly well known. For example, Marlan Scully discusses, in his book [1], a two-photon microscope scheme that beats the diffraction limitation by a factor of $\sqrt{2}$, by making a $\text{sinc}^4(kx)$ diffraction pattern instead of the usual $\text{sinc}^2(kx)$. Such narrowing of a diffraction pattern can be observed by a detector sensitive to the square of intensity, instead of just intensity itself. In other words, one needs a two-photon process to observe the $\sqrt{2}$ narrowing beyond the diffraction limit, even within classical optics. Moreover, using detectors based on a higher-order multi-photon process, which are sensitive exclusively to the higher orders of intensity, one could see even narrower diffraction patterns.

This approach would not work so well for holographic imaging used in lithography. In this technique, the desired image is composed of interference fringes of different spatial frequencies, so the resolution is given by the highest spatial frequency. This spatial frequency is equal to the inverse of the fringe period, which cannot be shorter than one half of the optical wavelength. It is easy to see that this period is the same for any power of intensity, for example, a $\text{sin}^4(kx)$ fringe has the same period as a $\text{sin}^2(kx)$ fringe.

Different approaches have been suggested to obtain an interference fringe of the square of the intensity with a shorter period. It has been proposed, for example, that frequency modulation can be used to blur the longer-wavelength component of a $\text{sin}^4(kx)$ fringe [2]. The use of quantum sources of light to beat this

* E-mail: Dmitry.V.Strekalov@jpl.nasa.gov

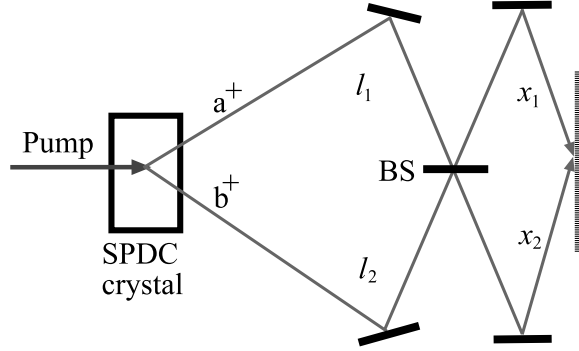


Figure 1. Two-photon interferometer with photosensitive substrate.

limit has also been proposed [3] and demonstrated with electronic coincidence detection [4].

Consider the setup in figure 1, which has been proposed for quantum interferometric lithography [3]. This is a modification of a well-known two-photon interference experiment [5, 6], in which the single-photon detectors are removed and the output beams are directed at a two-photon sensitive substrate (e.g. one covered with a lithographical photoresist).

Following the standard theoretical treatment for two-photon interferometers, we write the two-photon square amplitude as

$$|A|^2 \equiv \langle \Psi | \hat{E}^{(-)} \hat{E}^{(-)} \hat{E}^{(+)} \hat{E}^{(+)} | \Psi \rangle = |\langle 0 | \hat{E}^{(+)} \hat{E}^{(+)} | \Psi \rangle|^2, \quad (1)$$

where the fields depend on the propagation paths, and the state $|\Psi\rangle$ is the frequency-entangled output state of a Spontaneous Parametric Down Converter (SPDC):

$$|\Psi\rangle = \int d\nu h(\nu) \hat{a}^\dagger(\nu) \hat{b}^\dagger(-\nu) |0\rangle. \quad (2)$$

In equation (2), creation operators \hat{a}^\dagger and \hat{b}^\dagger refer to channels labelled l_1 and l_2 , respectively, in figure 1; ν is the frequency-detuning from the central frequency ω_0 , the latter being equal to one half of the pump frequency ω_p . The spectral function $h(\nu)$ gives the phase-matching width and accounts for inexact momentum conservation due to the finite length L of the crystal:

$$h(\nu) = \frac{1 - e^{-iL\Delta_z(\nu)}}{iL\Delta_z(\nu)}. \quad (3)$$

Derivation and analysis of expressions (2) and (3) are given in a number of publications on SPDC. In particular, in [7, 8], it is shown that for collinear degenerate type-I SPDC

$$\Delta_z(\nu) = -D'\nu^2, \quad D' = \left. \frac{d}{d\omega} \frac{1}{v} \right|_{\omega_0}, \quad (4)$$

and for collinear degenerate type-II SPDC, where the signal and idler photons have orthogonal polarizations, we have

$$\Delta_z(\nu) = D\nu, \quad D = \frac{1}{v_o} - \frac{1}{v_e}, \quad (5)$$

where v denotes the group velocity of the signal and idler photons. In case of orthogonal polarizations (type-II), the group velocity v has indices o and e for ‘ordinary’ and ‘extraordinary’ polarization components.

The two-photon amplitude of equation (1) can describe the coincidence detection rate, as well as the two-photon absorption rate, as a function of pathlengths $l_{1,2}$ and $x_{1,2}$. In the coincidence detection case, the fields in equation (1) are evaluated at the two distinct locations of the two detectors, while in the two-photon absorption case they are evaluated at the same, arbitrary, point on the photosensitive substrate. A geometric size of the ‘point’ in this context may be equal to the size of photo emulsion grain, or of the photoresist molecule. It is reasonable to assume that this size is much smaller than the interference structure we are expecting to see. As a further simplification, we will consider a one-dimensional problem with exactly counterpropagating beams. This geometry is obviously not practical, since no light energy is delivered to the surface, and we study this case just as an illustration allowing us to simplify the treatment.

As a next step, we need to represent the fields in (1) in terms of the same operators that describe the two-photon wavefunction, equation (2). For perfectly monochromatic plane waves with a wavenumber $k = \omega_0/c$, the representation is obtained by propagating the operators through the interferometer:

$$\hat{E}^{(+)} = \hat{a}e^{ikl_1} \left(\frac{1}{\sqrt{2}}e^{ikx_2} + \frac{i}{\sqrt{2}}e^{ikx_1} \right) + \hat{b}e^{ikl_2} \left(\frac{1}{\sqrt{2}}e^{ikx_1} + \frac{i}{\sqrt{2}}e^{ikx_2} \right). \quad (6)$$

In equation (6), the proportionality constant is placed between the field operator and the annihilation operator equal to unity. Also, it is assumed that the fields in the arms l_1 and l_2 have the same polarization. It is easy to see that otherwise there will be no two-photon interference fringes on the photosensitive substrate.

The plane-wave approximation implies that in the wave function equation (2), $h(\nu)$ should be replaced by $\delta(\nu)$. Then substituting equations (6) and (2) into equation (1) it is easy to see that the terms with \hat{a}^2 and \hat{b}^2 drop out, which is consistent with only one photon being present in each channel. The other four terms can be represented by four paths shown in figure 2. These paths correspond to both photons being transmitted by the beamsplitter (a), both reflected by it (b), one transmitted, the other reflected (c), and vice versa (d). Notice that, in the usual coincidence-detection treatment of two-photon interference, the amplitudes corresponding to paths (c) and (d) are discarded simply because they do not result in a pair of coincident detections. Therefore, one cannot directly apply to our system the well-known results for a two-detector experiment, and then argue that the detectors are placed at the same point, since this leads to loss of the amplitudes (c) and (d). Let us now show that it is these amplitudes that give rise to two-photon interference.

In the following, a more realistic model of wavepackets than plane waves is considered. The fields will be allowed to have a finite frequency bandwidth around the central frequency ω_0 , described by a real, even function $f(\nu)$:

$$E = \int d\nu f(\nu) \left\{ \hat{a}(\nu)e^{ik(\nu)l_1} \left(e^{ik(\nu)x_2} + ie^{ik(\nu)x_1} \right) + \hat{b}(\nu)e^{ik(\nu)l_2} \left(e^{ik(\nu)x_1} + ie^{ik(\nu)x_2} \right) \right\}. \quad (7)$$

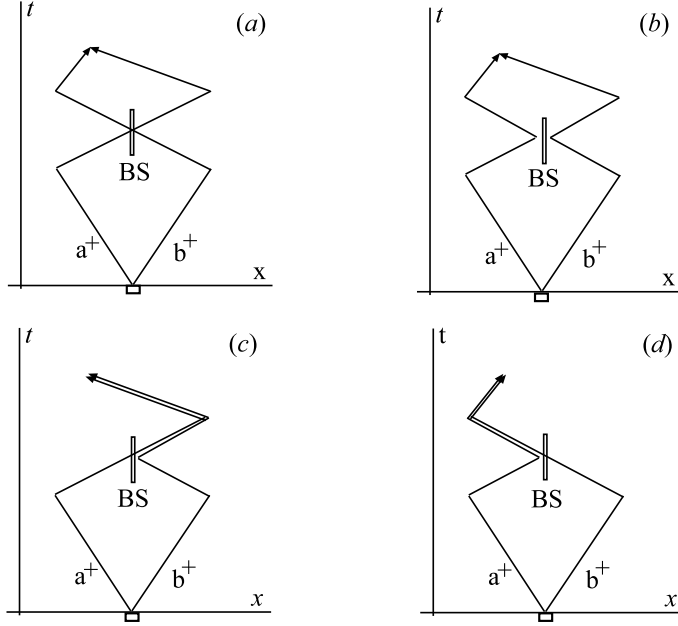


Figure 2. Different two-photon paths contributing to the amplitude (1): (a) both photons are transmitted; (b) both reflected; (c) transmitted–reflected; (d) reflected–transmitted.

Then the two-photon amplitude, equation (1), takes on the following form:

$$\begin{aligned}
 A = & \int d\nu d\nu_1 d\nu_2 h(\nu) f(\nu_1) f(\nu_2) \\
 & \times \left\{ e^{ik(\nu_1)l_1} e^{ik(\nu_2)l_2} \left(e^{ik(\nu_1)x_2} + ie^{ik(\nu_1)x_1} \right) \left(e^{ik(\nu_2)x_1} + ie^{ik(\nu_2)x_2} \right) \right\} \\
 & \times \langle 0 | \hat{a}(\nu_1) \hat{b}(\nu_2) \hat{a}^\dagger(\nu) \hat{b}^\dagger(-\nu) | 0 \rangle.
 \end{aligned} \tag{8}$$

The inner product in equation (8) is equal to $\delta(\nu_1 - \nu)\delta(\nu_2 + \nu)$ which reduces equation (8) to a single integral. To handle it, we expand $k(\nu) = k_0 + \nu/c$, where $k_0 \equiv k(\omega_0)$. This then gives

$$A = e^{ik_0(l+x)} [u(\Delta l + \Delta x) - u(\Delta l - \Delta x) + 2u(\Delta l) \cos(2k_0 \Delta x)], \tag{9}$$

where $u(z)$ is given by a Fourier transformation of a combined spectral density, and therefore has the meaning of a correlation function, namely,

$$u(z) \equiv \int d\nu h(\nu) f^2(\nu) e^{i(\nu/c)z}. \tag{10}$$

In equation (10), the variables $x \equiv x_2 + x_1$, $\Delta x \equiv \frac{1}{2}(x_2 - x_1)$, $l \equiv l_2 + l_1$ and $\Delta l \equiv l_2 - l_1$ have been introduced. Note that the coordinate along the substrate Δx is equal to a half of the path difference $x_2 - x_1$.

Analysing the symmetry properties of $h(\nu)$, it is found that in both cases of type-I, equation (4), and type-II, equation (5), SPDC $u(z)$ is always a real, even function:

$$u(z) = u(-z) = u^*(z) = u^*(-z). \tag{11}$$

Therefore, the first two terms in equation (9) cancel each other when $\Delta l = 0$. Taking the absolute square of the remaining term, we get

$$|A|^2 = 4u^2(0) \cos^2(2k_0\Delta x). \quad (12)$$

From equation (12) it can be seen that the two-photon absorption amplitude is a periodic function of coordinate Δx measured along the photosensitive substrate, that has a spatial frequency $4k_0$, which is twice the spatial frequency of the usual, second-order interference fringes. The two-photon interference fringes of equation (12) appear to have a perfect contrast for all Δx . This is a consequence of a plane-wave approximation *for the pump*. If one considers the pump with a finite bandwidth, the exponential pre-factor in (9) will no longer be just a phase factor, but will turn into an envelope, equivalent to the pump envelope. Therefore the two-photon interference fringes (12) will have a coherence length equal to the pump coherence length, which may be quite long and can reach metres for cw lasers.

It is very important that the two-photon coherence length does not depend on the bandwidth of the fields given by $f(\nu)$, nor on the phase-matching width given by $h(\nu)$. This is obvious from the condition $\Delta l = 0$. It has been shown [5, 6], that in this case the two-photon amplitudes represented in figure 2 by diagrams (a) and (b) exactly cancel each other, and the photon pair always goes to one channel (either x_1 or x_2), depicted in diagrams (c) or (d). In other words [3], the beamsplitter produces an entangled state, $|2\rangle_{x_1}|0\rangle_{x_2} - |0\rangle_{x_1}|2\rangle_{x_2}$, which picks up spatial phase at the same rate as the pump photon would. It also dephases at the same slow rate as the pump photon does, owing to its finite bandwidth, which results in the two-photon coherence length of the SPDC light being equal to the pump (single-photon) coherence length.

Now let us consider the linear interference in the apparatus. This analysis is important, since the modulations of intensity will directly affect the result equation (12) for the two-photon absorption rate. For example, there will be no two-photon absorption in the nodes of the single-photon interference fringe.

The expression for intensity is

$$I = \langle \Psi | \hat{E}^{(-)} \hat{E}^{(+)} | \Psi \rangle, \quad (13)$$

where the state $|\Psi\rangle$ is given by equation (2) and the field is given by equation (7). Setting $l_1 = l_2$, and treating this expression the same way we have treated the fourth-order field momenta, we arrive at

$$I = 1 - \cos(2k_0\Delta x) \int d\nu |h(\nu)|^2 f^2(\nu) \sin\left(2\frac{\nu}{c}\Delta x\right). \quad (14)$$

Notice that the integrand in equation (14) is an odd function, and hence the whole integral is zero and equation (14) equals unity. This means that in our apparatus there will be no intensity modulations due to the second-order interference, regardless of the individual coherence length of the signal and idler photons. This at first appears surprising, since one might expect to see at least a few interference fringes at the white light interference condition $x_1 = x_2$. However, taking into account that both inputs of the beamsplitter are used, there are two sets of interference fringes exactly out of phase with each other, and hence the total intensity is unmodulated.

Two more issues associated with two-photon quantum imaging need to be addressed to make it a practically useful technology. One is the availability of two-photon sensitive photoresists and detectors, and the other has to do with the fact that using SPDC as a two-photon source, one first loses a factor of two in spatial resolution by downconverting the pump frequency (and hence doubling the wavelength), and then regain this factor by using two-photon processes. Therefore, in terms of spatial resolution, the quantum imaging technique has no apparent advantage over using classical imaging at the pump wavelength. The counter is that it is not always possible to use the UV light argument [9]. For example, it may be incompatible with imaging biological or other light sensitive objects. Another example is 3D lithography [9]. Creating 3D structures with single-photon exposure of photolithographical materials is very difficult, since they strongly absorb UV light, which limits the depth of penetration. Two-photon exposures solve this problem. However, much value would be added to the quantum imaging technology if one could prepare two-photon states without doubling the wavelength. One way to achieve it is to use a Hyper Parametric Scattering (HPS) instead of SPDC.

HPS is a nonlinear optical process occurring via the cubical optical nonlinearity $\chi^{(3)}$, in which *two* pump photons recombine into an entangled photon pair. This process is similar to four-wave mixing in the same sense as SPDC is similar to parametric amplification (PA): four-wave mixing and PA assume non-vacuum input into the signal or the idler modes. HPS is distinct from the SPDC, where a *single* pump photon produces an entangled pair. This distinction is most evident from comparing the phase-matching conditions for SPDC with those for HPS:

$$\vec{k}_p = \vec{k}_s + \vec{k}_i, \quad \omega_p = \omega_s + \omega_i, \quad (15)$$

$$2\vec{k}_p = \vec{k}_s + \vec{k}_i, \quad 2\omega_p = \omega_s + \omega_i, \quad (16)$$

which is illustrated graphically in figure 3. An important thing to notice in figure 3 is that the average wavelength of the photons produced in HPS is the same as that of the pump, while in the case of SPDC it doubles.

HPS was observed for the first time over 30 years ago [10]. At that time, it did not attract attention as a source of EPR-states because of a very low efficiency of the $\chi^{(3)}$ processes compared to $\chi^{(2)}$ processes. A typical value for $\chi^{(2)}$ is 10^{-8} statvolt $^{-1}$, while for $\chi^{(3)}$ it is 10^{-15} statvolt $^{-2}$. Fortunately, HPS output power is quadratic with respect to the pump intensity, while in the case of SPDC it is

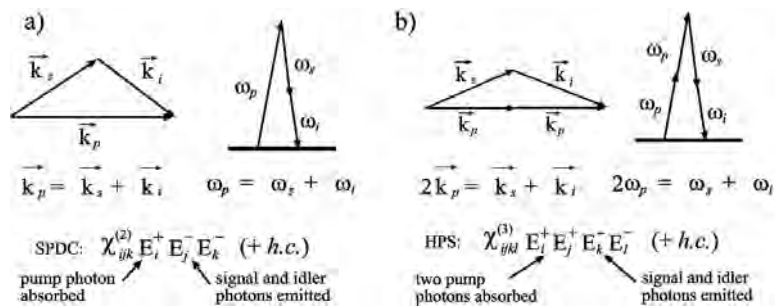


Figure 3. The phase-matching (momentum and energy conservation) diagrams for SPDC (a) and HPS (b).

only linear. To compare efficiencies of the two processes, one must compare the $|E_p\chi^{(2)}|$ and $|\chi^{(3)}|$. Modern powerful femtosecond lasers, that were not available in the early days of HPS, dramatically changed the situation in favour of HPS.

Another argument in favour of HPS is that, unlike SPDC, this process does not require any particular symmetry of the media and can be observed not only in crystals but also in glass fibres [11], which promises to increase the interaction length to metres or beyond. Furthermore, it has been shown [12] that nearly four orders of magnitude improvement of the signal can be achieved by cascading two $\chi^{(2)}$ processes to emulate a $\chi^{(3)}$ HPS process. A large amount of research has been done on $\chi^{(3)}$ processes, and particularly on four-wave mixing [1, 13–15], and we plan to rely on these results in a new research programme directed at creating a robust source of entangled photon pairs or two-photon states without down-converting from a higher frequency.

The second practical issue, mentioned above, is the availability of two-photon sensitive photoresists. Considering the very low power of two-photon sources, a high two-photon sensitivity of the photoresists is required. Unfortunately, high, single-photon, UV sensitivity of many commercially available photoresists does not guarantee that they would be suitable two-photon sensitive materials. The synthesis of such a material appears to be a difficult task, although a large volume of research has been done in this area motivated by the growing recognition of the two-photon imaging technology importance [9, 16, 17].

We also have carried out a preliminary search for two-photon sensitive lithographic materials. Relying on the analogy with atomic systems, we expect that a suitable two-photon material would have an intermediate level corresponding to the single-photon energy, so that the single-photon detuning, which factors inversely into the two-photon absorption cross-section, is small, and the two-photon absorption rate is peaked. It is further required that the molecular transition corresponding to the intermediate absorption level does not result in photochemical reaction in photoresist (otherwise the resist would be one-photon sensitive). Finally, we require that the intermediate level or band is normally depopulated and very short-lived (otherwise the resist would be one-photon sensitive via cascaded processes); and that both transitions have the correct selection rules.

We have taken absorption spectra of various commercially available photoresists. The results are shown in figure 4. One of our samples, the Novalac 5740, has shown a local absorption maximum which is centred at about 520 nm and is clearly separated from the strong transition in the UV part of the spectra, which is associated with the photochemical reaction initiating the photoresist. We spun an approximately 15 μm thick sample of this photoresist on a gold plated substrate and exposed the sample to different doses of argon ion laser light, whose wavelength (514.5 nm) was close to the centre of the absorption peak of interest. A threshold dose of about 2 kJ/cm², was found, assuming 100% radiation reflection off the mirror substrate and operating at the intensity level of 5 W/cm². Repeating the experiment at 25 W/cm², gave the same results with an exposure time that was five times shorter. This result suggests that the exposure process is linear in intensity and hence is a single-photon one. Notice that the threshold found at 514.5 nm is roughly five orders of magnitude higher than for a regular UV exposure.

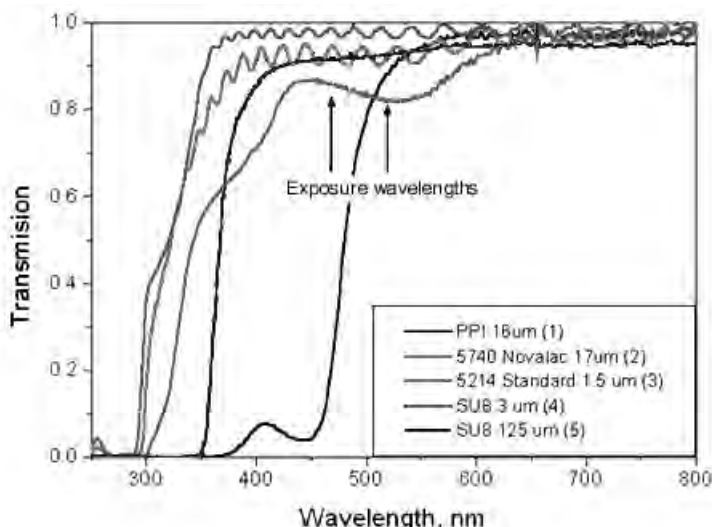


Figure 4. Absorption spectra for different photoresists. The sample of choice shows an absorption maximum centred at about 520 nm. Arrows mark the wavelengths the sample was exposed to: 457.9 nm and 514.5 nm.

Next, the exposures were repeated for another argon ion laser line with 457.9 nm wavelength, which is off the intermediate absorption peak but is closer to the UV absorption transition. It was found that, at this wavelength, the threshold dose was definitely lower than 0.4 kJ/cm^2 . This suggests that the high-threshold photo-initiation observed at 514.5 nm, as well as at 457.9 nm, is not related to the intermediate absorption peak, but rather is due to a far off-resonant absorption on the wing of the UV absorbing transition. Therefore, the selected material may satisfy the above-outlined requirements for a two-photon optimized photoresist, and it would be interesting to try exposing it with a two-photon source. We plan on carrying out such experiment in the near future.

In conclusion, a rigorous analysis has been carried out that confirmed the earlier results [3]. In addition, the analysis has shown that the desired two-photon interference fringe will have a very long coherence length, equal to that of the pump, and that the second-order (single-photon) interference fringes will be entirely absent. The questions related to alternative sources of two-photon states and to the choice of two-photon sensitive photolithographical materials have been discussed. Although bringing the research in this area to the level of practical technology is a challenging task, it is at the same time an interesting and potentially rewarding one.

Acknowledgments

We would like to acknowledge useful discussions with R. Y. Chiao, J. D. Franson, D. F. V. James P. G. Kwiat, W.D. Phillips, Y. H. Shih, J. E. Sipe, and A. M. Steinberg. We thank Victor White for valuable help with photoresists. We also acknowledge financial support from the National Aeronautics and Space Administration, the Office of Naval Research, and the Advanced Research and Development Activity.

References

- [1] SCULLY, M. O., and ZUBAIRY, M. S., 1997, *Quantum Optics* (Cambridge: Cambridge University Press).
- [2] YABLONOVITCH, E., and VRIJEN, R. B., 1999, *Opt. Eng.*, **38**, 334.
- [3] BOTO, A. N., KOK, P., ABRAMS, D. S., BRAUNSTEIN, S. L., WILLIAMS, C. P., and DOWLING, J. P., 2000, *Phys. Rev. Lett.*, **85**, 2733–2736.
- [4] D'ANGELO, M., CHEKHOVA, M. V., and SHIH, Y. H., 2001, *Phys. Rev. Lett.*, **87**, 013602.
- [5] HONG, C. K., OU, Z. Y., and MANDEL, L., 1987, *Phys. Rev. Lett.*, **59**, 2044–2046.
- [6] SHIH, Y. H., and ALLEY, C. O., 1988, *Phys. Rev. Lett.*, **61**, 2921–2924.
- [7] SHIH, Y. H., SERGIENKO, A. V., RUBIN, M. H., KIESS, T. E., and ALLEY, C. O., 1994, *Phys. Rev. A*, **50**, 23–28.
- [8] BURLAKOV, A. V., CHEKHOVA, M. V., KLYSHKO, D. N., KULIK, S. P., PENIN, A. N., SHIH, Y. H., and STREKALOV, D. V., 1997, *Phys. Rev. A*, **56**, 3214–3225.
- [9] BELFIELD, K. D., SCHAFTER, K. J., LIU, Y., LIU, J., REN, X., and VAN STRYLAND, E. W., 2000, *J. Phys. Org. Chem.*, **13**, 837–849.
- [10] WEINBERG, D. L., 1969, *Appl. Phys. Lett.*, **16**, 32.
- [11] KUMAR, P., and KOLOBOV, M. I., 1994, *Opt. Commun.*, **104**, 374.
- [12] KLYSHKO, D. N., 1988, *Photons and Non-linear Optics* (New York: Gordon and Breach Science).
- [13] SLUSHER, R. E., HOLLBERG, L. W., YURKE, B., MERTZ, J. C., and VALLEY, J. F., 1985, *Phys. Rev. Lett.*, **55**, 2409.
- [14] NAGASAKO, E. M., BOYD, R. W., and AGARWAL, G. S., 1997, *Phys. Rev. A*, **55**, 1412.
- [15] BOYD, R. W., and AGARWAL, G. S., 1999, *Phys. Rev. A*, **59**, R2587.
- [16] BORISOV, R. A., DOROJKINA, G. N., KOROTEEV, N. I., KOZENKOV, V. M., MAGNITSKII, S. A., MALAKOV, D. V., TARAZISHIN, A. V., and ZHELTIKOV, A. M., 1998, *Appl. Phys. B*, **67**, 765.
- [17] JOSHI, M. P., PUDAVAR, H. E., SWIATKIEWICZ, J., PRASAD, P. N., and REINHARDT, B. A., 1999, *Appl. Phys. Lett.*, **74**, 170.